Optical spectroscopic ultrasound displacement imaging: a feasibility study

Tingyang Duan, Hengrong Lan, Hongtao Zhong, Meng Zhou, Ruochong Zhang, and Fei Gao*, *Member IEEE*

***Abstract*—Photoacoustic imaging has been intensively studied in recent years and many of the achievements have already been applied in clinical diagnosis and therapy, e.g. use spectroscopic photoacoustic imaging to extract functional and molecular information. However, spectroscopic photoacoustic imaging requires expensive and bulky tunable laser source, which severely hinder its further development towards portable device. In this paper, we propose a novel imaging method, named optical spectroscopic ultrasound displacement (OSUD) imaging, which enables optical spectroscopic imaging in deep scattering tissue using multiple low-cost continuous-wave laser sources and ultrasound imaging equipment. The principle of the OSUD imaging method will be introduced, followed by preliminary experimental results. The OSUD imaging may exploit the deep penetration merit of ultrasound, and provide another pathway to provide spectroscopic optical absorption contrast in deep scattering tissue beyond commonly used photoacoustic imaging, which will be further validated in the future work.**

***Index Terms*—Optical spectroscopic characterization, photoacoustic imaging, ultrasound displacement imaging, speckle tracking**

I. Introduction

Photoacoustic (PA) imaging is a fast-developing noninvasive imaging technique based on photoacoustic effect [1-6]. In PA imaging, ultrasound signals induced by pulsed laser illumination are detected to reconstruct 2-D or 3-D images. In recent decade, PA imaging has drawn much attention in biomedical applications for its deep penetration due to ultrasound detection and functional imaging capability due to optical absorption contrast, which is extremely demanding for accurate diagnostics and early treatment [7-12]. To perform PA imaging, two kinds of system setups are usually adopted: PAT (PA tomography) and PAM (PA microscopy). However, both of the systems are limited by expensive and bulky laser sources with tunable wavelength and high peak power, which renders the conventional PA imaging system impossible to be portable and low-cost. Although some efforts have been done to overcome this problem such as utilizing laser diodes, the development of laser-diode-based PA systems are severely limited by its lower pulse energy compared with high-power lasers [13, 14]. To the best of our knowledge, the high-cost issue of pulsed tunable laser source in PA imaging has been an open challenge in this community to be solved.

In this paper, a new imaging method, named optical spectroscopic ultrasound displacement (OSUD) imaging, will be introduced and experimentally verified. In OSUD imaging, multiple continuous-wave (CW) lasers with different wavelengths are utilized to illuminate the sample, resulting in localized heating and temperature rising. Such localized temperature rising will induce acoustic velocity change, which could be captured by ultrasound displacement imaging before and after the laser heating through speckle tracking algorithm. By step-to-step tracing back from the OSUD images to the original optical absorption coefficient, this method will reflect the relative optical spectroscopic characterization of target samples. Therefore, the proposed OSUD imaging method enables multi-wavelength optical absorption contrast using conventional pulse-echo ultrasound imaging with high spatial resolution and deep penetration. It deserves noting that the proposed OSUD imaging transforms the requirement for an expensive tunable pulsed laser source to multiple low-cost CW lasers together with an ultrasound imaging device. In the following sections, the theory and analytical model will be introduced first, experimental results are then illustrated for supporting the model and method.

II. Principle and Method

In traditional PA imaging systems, the sample is irradiated by a short-pulse laser source, giving rise to temperature elevation and PA signal generation due to optical absorption of the samples. The generated PA signals could be detected by ultrasound transducers for image reconstruction. Just like PA imaging, the proposed OSUD imaging method also utilizes laser sources to illuminate the sample. As shown in Fig. 1, here we apply CW lasers to induce localized temperature rising in the sample, but not PA signals. Lasers will be turned on between two transmitting ultrasound signals and correspondently we can receive two echo signals. By mechanically scanning and data acquisition, B-mode ultrasound images before and after heating will be reconstructed. OSUD images are obtained by applying speckle tracking algorithm for post-processing and spectroscopic analysis. From the previous literatures [15], the temperature rising $\Delta T(\lambda_i)$ caused by laser illumination with wavelength

Tingyang Duan Hengrong Lan, Hongtao Zhong, Meng Zhou and Fei Gao are with the School of Information Science and Technology, ShanghaiTech University, Shanghai 201210, China (*e-mail: gaofei@shanghaitech.edu.cn)

Ruochong Zhang is with the School of Electrical and Electronic Engineering, Nanyang Technological University, Singapore 639798.

λ_i (i means multiple laser sources and is used to represent different wavelengths) could be expressed as:

$$\Delta T(\lambda_i) = \frac{\eta_{th} A_e(\lambda_i)}{\rho C_V} = \frac{\eta_{th} \mu_a(\lambda_i) F}{\rho C_V} \quad (1)$$

where η_{th} denotes the energy conversion efficiency from light to heat, $A_e = \mu_a(\lambda_i)F$ is the optical energy deposition density with optical fluence F and optical absorption coefficient $\mu_a(\lambda_i)$, ρ is the mass density, and C_V represents the specific heat capacity at constant volume. From Eq. (1), we could observe that the temperature rise is directly related to optical absorption coefficient at specific wavelength $\mu_a(\lambda_i)$.

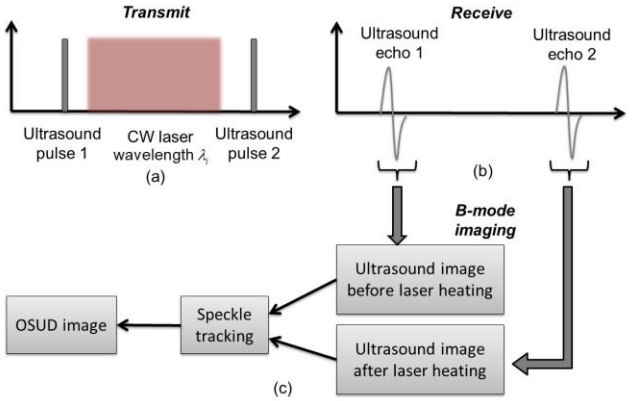

Fig. 1 (a) Transmit signal pattern, including two ultrasound pulses before and after CW laser illumination. (b) The received pulse-echo ultrasound signals. (c) Image reconstruction process including B-mode imaging of ultrasound signals before and after CW laser heating, followed by speckle tracking algorithm.

Next, we need to relate the temperature rise with the acoustic velocity variation, which could be measured by ultrasound displacement imaging that has been explored to monitor the temperature in previous literatures [17-20]. Specifically, acoustic velocity $v_t(\lambda_i)$ increases with rising temperature when the sample is heated up by the CW laser illumination. Some polynomial or exponential model are used to depict the relationship between temperature and speed of sound. However, in a small range of temperature variation (0~10℃), this can be simplified to a linear relation. This linear model is adopted in this paper because we strictly controlled the heating time to avoid overheating and damaging inside samples. This is also practical to the future *in vivo* experiment for the reason that the incident light intensity should not excess the ANSI limit (20 mJ/cm^2) to prevent any damage of tissues. Therefore the relationship could be expressed by the below equation [23, 24]:

$$v_t(\lambda_i) = v_i + a\left(T_{at} + \Delta T(\lambda_i)\right) = v_i + a\left(T_{at} + \frac{\eta_{th}\mu_a(\lambda_i)F}{\rho C_V}\right) \quad (2)$$

Where v_i is the acoustic velocity of the medium at 0 ℃, a is the coefficient relating temperature and acoustic velocity increase, and T_{at} is the ambient temperature (e.g. 25 ℃), ΔT is the transient temperature rise due to the CW laser illumination. The acoustic velocity variation in above equation can be characterized by the time delay difference Δt_{delay} between two pulse-echo ultrasound signals before and after CW laser illumination. Assuming a cylindrical absorbing sample such as a tube injected with ink, the time delay difference could be simply expressed as:

$$\Delta t_{delay} = t_{delay1} - t_{delay2} = d_r\left[\frac{1}{v_t} - \frac{1}{v_t(\lambda_i)}\right] \quad (3)$$

Where t_{delay1} and t_{delay2} are the time delays of pulse-echo ultrasound signals before and after CW laser illumination, d_r is the sample diameter. By substituting the equation (2) into (3), an explicit equation is obtained to describe the relationship between time delay and optical absorption coefficient.

$$\begin{aligned}
\Delta t_{delay} &= d_r\left[\frac{1}{v_i + aT_{at}} - \frac{1}{v_i + a\left(T_{at} + \Delta T(\lambda_i)\right)}\right] \\
&= d_r\left[\frac{1}{v_i + aT_{at}} - \frac{1}{v_i + a\left(T_{at} + \frac{\eta_{th}\mu_a(\lambda_i)F}{\rho C_V}\right)}\right] \\
&= d_r\left[\frac{\frac{a\eta_{th}\mu_a(\lambda_i)F}{\rho C_V}}{\left(v_i + aT_{at}\right)^2 + a\left(v_i + aT_{at}\right)\frac{\eta_{th}\mu_a(\lambda_i)F}{\rho C_V}}\right] \\
&\approx d_r\left[\frac{a\eta_{th}\mu_a(\lambda_i)F}{\left(v_i + aT_{at}\right)^2 \rho C_V}\right], \text{when } \left(v_i + aT_{at}\right) ? \ \frac{a\eta_{th}\mu_a(\lambda_i)F}{\rho C_V} \\
&= \Gamma\mu_a(\lambda_i)F, \text{where } \Gamma = d_r\frac{a\eta_{th}}{\left(v_i + aT_{at}\right)^2 \rho C_V}
\end{aligned} \quad (4)$$

There is an approximation in the fourth step due to a small time increment and coefficient α, which is far smaller than the velocity at 0 ℃ (~1450m/s). From above equation, we could observe that the time delay difference $\Delta t_{delay} = \Gamma\mu_a(\lambda_i)F$ is linearly proportional to the optical absorption coefficient $\mu_a(\lambda_i)$ at specific CW laser wavelength λ_i.

Speckle tracking algorithm [22, 25] is applied based on the steps in Table 1. Two B-mode images are processed as reference image and candidate image respectively. This algorithm is used to calculate the minimum SAD (Sum of Absolute Difference) in candidate image to match the most similar pixel in reference image. Hence the displacement between two pixels can be obtained.

According to the derivation demonstrated above, the OSUD method can be presented in Fig. 2 using a flowchart. Combining with displacement images and speckle tracking algorithm, the spectroscopic characterization of target samples can be finally acquired through this tracing back flow diagram,

Table 1 Speckle tracking algorithm used for obtaining displacement

Algorithm 1 Speckle Tracking

Input: Two B-mode images
Output: OUSD image

```
Begin
Initialize size of Template Block and Search Window.
repeat
    for pixel=start:end(within search window) do
        Calculate and Record SAD
    end for
    Find the minimum value of SAD and obtain displacement
    Move to next pixel(within image)
until Last pixel of image
return OUSD Image
```

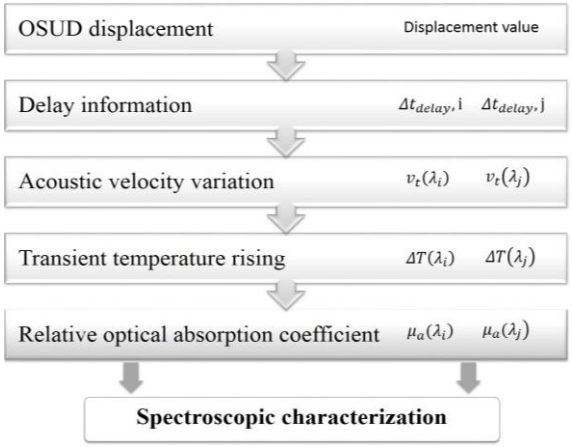

Fig.2 OSUD method: Trace back from the displacement to the relative optical absorption coefficient.

which can provide multi-wavelength optical absorption contrast using ultrasoud images.

Specifically, we need to reconstruct the images based on the obtained pulse-echo ultrasound signals before and after CW laser illumination, as shown in Fig. 1(c). It is known that time delay differences in the ultrasound signals lead to the speckle displacement in the reconstructed B-mode ultrasound images. Therefore, we firstly reconstruct the two ultrasound images before and after CW laser illumination, and then perform speckle-tracking algorithm in small area of interest to compare these two images to acquire the final OSUD image. Experimental results will be compared with the spectroscopic curves measured by UV-VIS spectroscopy for proof of concept.

III. Setups and Materials

The experimental setup to prove the concept of OSUD imaging is shown in Fig. 3. To perform the proposed OUSD method, multi-CW lasers will be firstly utilized. It included three CW lasers (peak power: 1 W) with different wavelengths (e.g. 671 nm, 808 nm, and 980 nm in this experiment) coupled with multi-mode fibers (core diameter: 400 μm). The fiber couplers were detachable for easy operation of switching these CW lasers. Signal generator is exploited to controll the on-off state of CW lasers. At the output of the fiber, two condenser lens were utilized to collimate and focus the light on the sample in a water tank. The focal spot was adjustable depending on the resolution requirement. A focused ultrasound transducer (I10C8F20, Doppler Inc.) with 1 cm diameter and 10 MHz central frequency was immersed in the water tank, and adjusted to be confocal with the laser focal spot. The transducer was connected to pulser-receiver (5072PR, Olympus) to transmit and receive pulse-echo ultrasound signals. Both the fiber tip, condenser lens, and ultrasound transducer were mounted to a mechanical scanner driven by step motor. The received ultrasound signals were digitized by

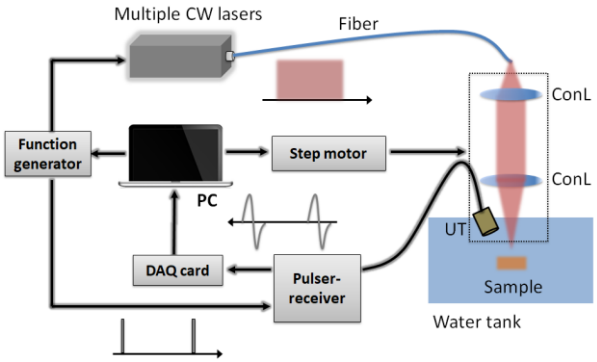

Fig. 3 Experimental setup of the OSUD imaging. CW: continuous wave; ConL: condenser lens; UT: ultrasound transducer; PC: personal computer; DAQ: data acquisition.

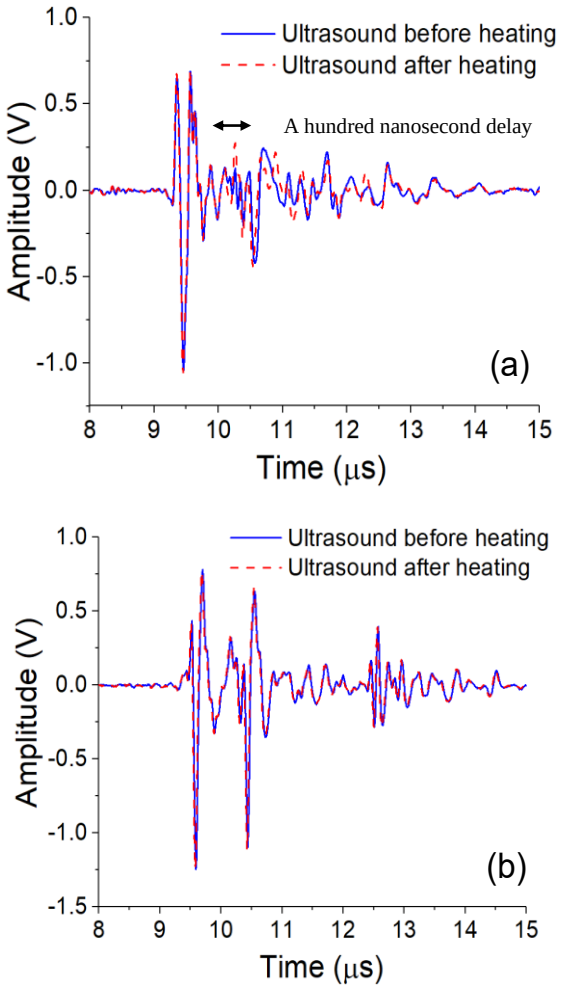

Fig. 4 (a) Pulse-echo ultrasound signals from tube filled with blue ink before (solid blue line) and after (dashed red line) CW laser heating (671 nm wavelength). (b) Pulse-echo ultrasound signals from tube filled with water before and after CW laser heating.

a data acquisition (DAQ) card (9814, AD Link) with 80 MSPS sampling rate. A computer was used to synchronize the whole system including raster scanning, ultrasound transmission, CW laser illumination, and DAQ data capture sequentially.

It deserves noting that the CW laser illumination needs to be properly placed between two sets of ultrasound transmission/receiving. In this experiment, the laser heating period was selected as 1 ms to guarantee sufficient heating while preventing the damage of the sample. The trigger of second ultrasound transmission immediately after CW laser heating was tuned to be within 1 μs so that thermal diffusion could be neglected. In the preliminary experiments, the sample is made of three transparent silicone tubes (2 mm diameter) filled with water, blue ink and gold nanorod solution respectively, which are supposed to exhibit similar ultrasound reflection but significantly different optical absorption at near-infrared wavelength range.

IV. Results

Four experiments were conducted to verify the proposed OSUD method. Firstly the time-domain pulse-echo waveforms of pure water and blue ink are showed to explain that optical absorption may change or remain stable after illuminated by laser source according to the diversity of sample material and optical property. Two groups of depth information of samples are given as cross-section images, which shows the delay difference before and after heating from the angle of single point of samples' surface. Then from the average perspective, two groups of 2D images are illustrated to show displacement of samples. Finally by applying our OSUD method and tracing back to find the optical absorption difference, spectroscopic characterization of target samples can be obtained and compared to the real spectroscopic curves. A conclusion can be drawn that this OSUD method can improve optical absorption contrast and be promising for designing future low-cost and potable imaging system due to the results mentioned above

The time-domain waveform of pulse-echo ultrasound signal from the tube filled with blue ink is shown in Fig. 4(a). The blue solid line shows the pulse-echo ultrasound signal before CW laser heating (671 nm wavelength), while the red dashed line is the pulse-echo ultrasound signal after CW laser heating. Specially, Figure 4 (a) shows about a hundred nanoseconds' ultrasound delay in the signal level. This time-domain waveform has mainly two separated pulse-echo ultrasound signals. The first signal (at the domain of 9-10μs) denotes the echo ultrasound from the upper surface of the tube, which shows no difference because of no acoustic velocity change. The second signal (at the domain of 10-11μs) denotes the echo ultrasound from the bottom of the tube, which is influenced by acoustic velocity change due to temperature rising induced by optical absorption of the injected ink. A hundred nanoseconds' delay would be observed by comparing the second part of two curves. Due to the optical absorption of CW laser illumination and temperature rising, two ultrasound signals differ a lot, which is equivalent to speckle change in the reconstructed B-mode ultrasound images. On the other hand, the two ultrasound signals before and after CW laser heating are almost same for the tube filled with water, as shown in Fig. 4(b), which indicates an negligible optical absorption of water at 671 nm wavelength.

Through mechanical scanning, the cross-sectional images of the two silicone tubes (2 mm diameter) filled with blue ink and gold nanorod solution could be reconstructed using three CW lasers with different wavelength (671 nm, 808 nm, 980 nm). It is worth reminding that the heating time and output power using three laser sources are strictly controlled to be the same so that the optical fluence F can be stable and unchanged. In this experiment, CW laser illumination needs to be properly placed between two sets of ultrasound transmission/receiving. The laser heating period was selected as 1 ms to guarantee sufficient transient heating. As shown in Fig. 5, the cross-section ultrasound images before CW laser heating (Fig. 5(a)-(c)) and after laser heating (Fig. 5(d)-(f)) are revealing the two tubes obviously with similar image contrast. By performing speckle tracking to extract the speckle change, the proposed OSUD images (Fig. 5(g)-(i)) demonstrated distinct image contrast with different CW laser wavelength. Specifically speaking, the optical absorption of blue ink decreases with longer wavelength, while the optical absorption of gold nanorod solution increases. This could also be observed through the intensity distribution figures (Fig. 5(j)-(l)). These figures have been normalized to the same scale so that some detailed information like maximum relative intensity and contrast capability could be easily obtain. When comparing with different heating wavelength at same sample, the trend is clear that blue ink is gradually down while gold nanorod solution is increasing. For example, tube with gold nanorod solution will have a small maximum value and tiny intensity distribution after 671nm CW laser heating while a stronger intensity distribution and maximum value after 808nm CW laser heating. As for contrast between samples, the two tubes have a close intensity distribution after 671nm illumination and a wide difference after 808nm or 980nm heating, which is the foundation for discrimination. Cross-section images give intuitional results regarding the samples' surface. Another set of 2-dimensional ultrasound images are illustrated in Fig 6(a)-(i) after post-processing the receiving ultrasound data. Tubes are placed parallel and two rows of 2D B-Mode images are showed. Ultrasound images are obtained before and after laser heating and no direct displacement can be observed immediately in Fig. 6(a)-(f). The last row (Fig 6(g)-(i)) shows that the 2D OSUD images can provide displacement information: The largest contrast is located at gold nanorod solution tube in Fig. 6(h), giving an obvious displacement than blue ink tube after heating using a 808nm CW laser source. Similar displacement are showed in Fig. 6(i) between two tubes while gold nanorod solution has slightly larger displacement than blue ink after illumination by 980 nm CW laser. These 2D images provide proofs for supporting the cross-section comparison results in a more comprehensive way.

Lastly, by applying the proposed OSUD method, linking the displacement to optical absorption coefficient will allow us to

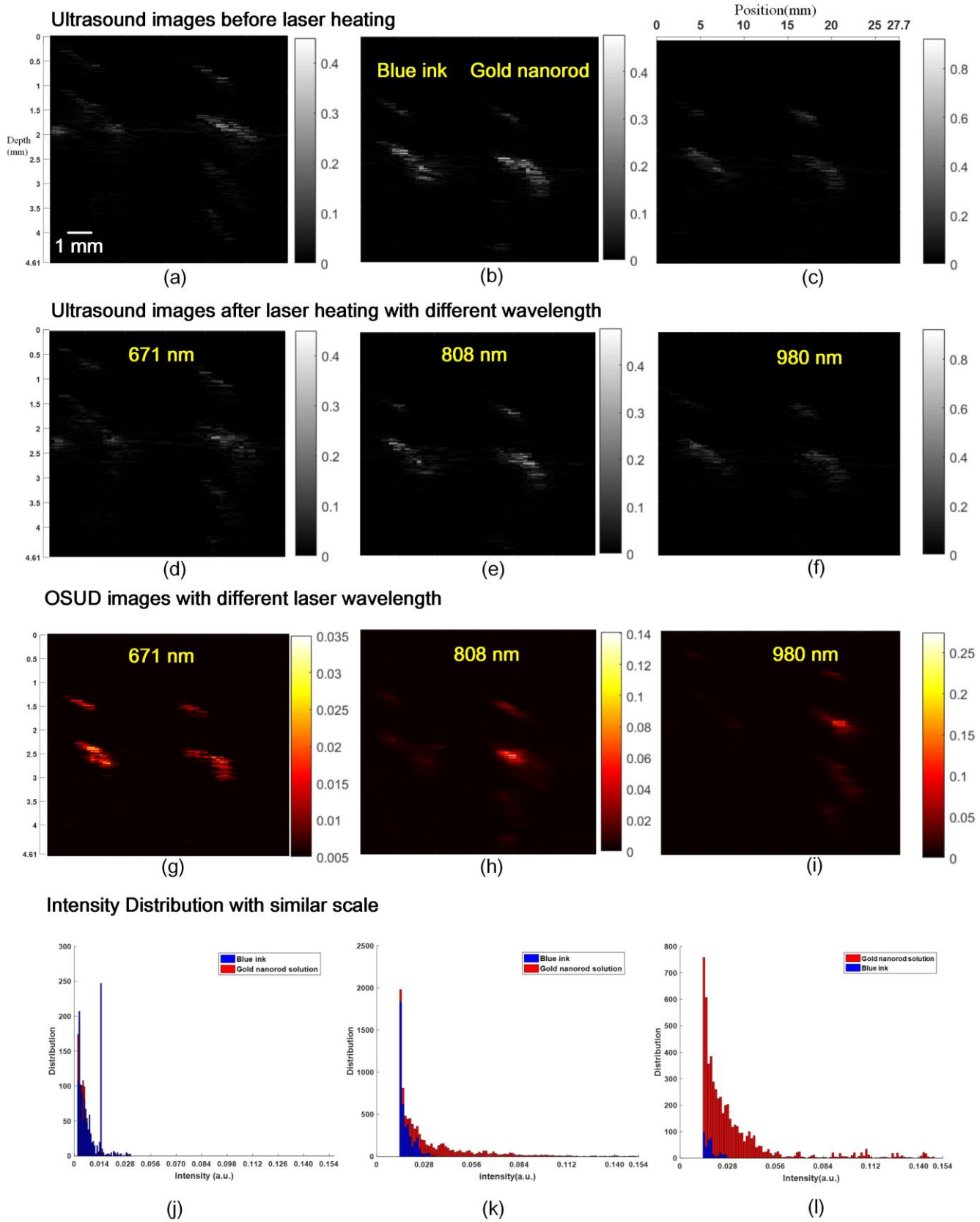

Fig. 5 (a)-(c) B-mode ultrasound images of two tubes filled with water and blue ink before CW laser heating, and (d)-(f) after laser heating with three different wavelengths: 671 nm, 808 nm, 980 nm. (g)- (i) OSUD images at these three wavelengths. (j) – (l) Intensity distribution at three wavelength.

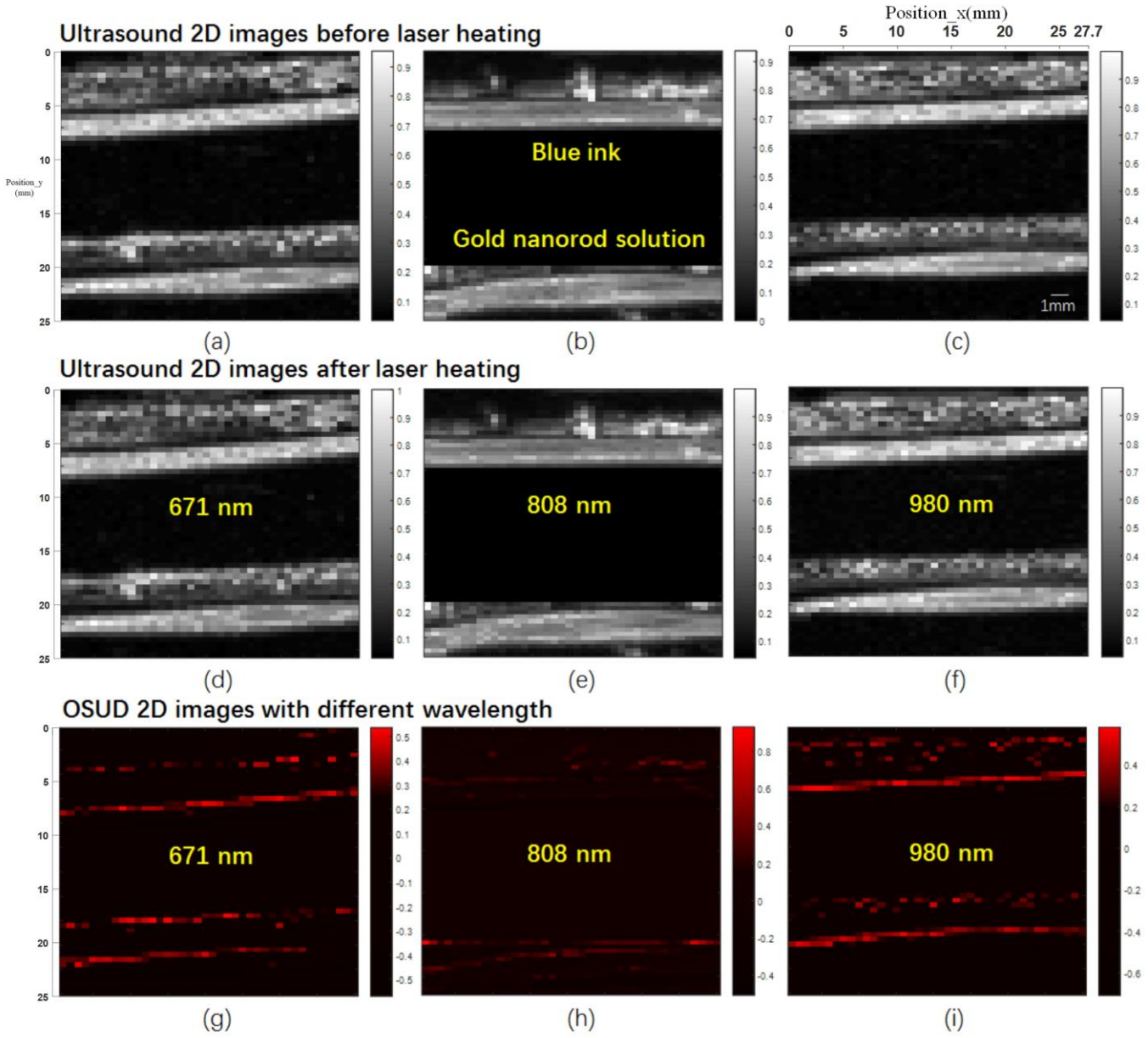

Fig. 6 (a)-(c) 2D ultrasound images of two tubes filled with gold nanorod solution and blue ink before CW laser heating, and (d)-(f) after laser heating with three different wavelengths: 671 nm, 808 nm, 980 nm. (g)- (i) OSUD 2D images at these three wavelengths.

obtain their spectroscopic characterization at different wavelength. Due to the merit of the proposed OSUD imaging method, red and blue points show that the optical absorption intensity of blue ink and gold nanorod solution have opposite trend at these three wavelength. With proper data normalization, we can easily find that the blue ink tube has stronger optical absorption than gold nanorod solution at 671nm, but weaker absorption at 808 and 980nm, which agrees well with the standard optical absorption spectrum measured by UV-VIS spectroscopy in Fig 7(a). From the perspective of image contrast, the conventional B-mode ultrasound images shows limited contrast due to the similar mechanical impedance of two silicon tubes filled with different liquids (Fig. 7(b) left). However, the proposed OSUD imaging method exhibits optical absorption contrast, which is more than 10 times higher at 808 nm wavelength than the conventional B-mode ultrasound imaging (Fig. 7(b) right).

V. Discussion and Conclusion

It deserves noting that the sensitivity of the proposed OSUD method in biomedical applications is fundamentally limited by the allowed temperature rise during the CW laser heating. According to the previous literatures regarding ultrasound measurement of temperature [18-20], ~0.1 degree of temperature rising could be reliably detected by ultrasound imaging, which is well within the allowed bio-safety region. Another concern is the influence of the tissue motion when performing the OSUD imaging, which could potentially be avoided by utilizing state-of-the-art ultrasound imaging machine to minimize the time required of two B-mode imaging

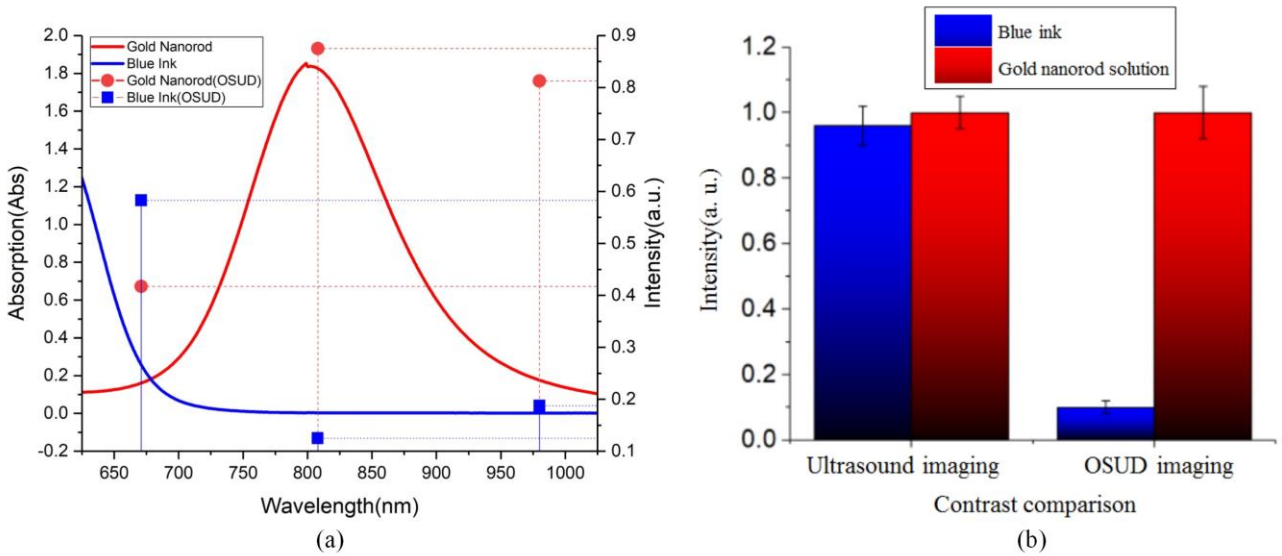

Fig. 7 (a) the optical absorption spectrum reconstructed from the proposed OSUD imaging method and the standard spectrum measured by spectroscopy. (b) The image contrast comparison between conventional B-mode ultrasound and the proposed OSUD imaging method.

procedures.

Though derivation about the displacement difference linking to optical absorption coefficient in the second section was done, the final expression of the modelling (Eq. (3)) is limited to cylindrical-like samples. One of the future work we can do is to further develop more complex analytical model to be applied in a more broaden and complicated situation. The accuracy of the speckle tracking algorithm can approach up to 95% according to the literature [22]. The dominant displacement direction is Y-axis in 2D images. In this literature, time delay before and after heating is at nanosecond level, equivalent to a micrometer displacement, which takes up 0.2λ (λ: the acoustic wavelength in water) displacement in Y direction. This displacement will ensure a desirable accuracy by applying speckle tracking algorithm.

Due to the random scattering of photons, it is difficult to estimate the light attenuation and distribution accurately in deep heterogeneous tissues. This issue is therefore becoming an open challenge in photoacoustic field that needs to be solved. Two main methods are under development tailored for breaking this barrier. One is the guided wavefront-shaping that is used to improve the light focusing in scattering tissue and achieve uniform fluence distribution in deep tissues [26, 27]. Another possible method is called Eigenspectra optoacoustic tomography developed by Vasilis et al [28], which can estimate the quantitative fluence distribution in deep tissue. In our future work, more accurate estimation of light fluence in deep tissue will be studied and performed to enhance the imaging capability of the OUSD method.

In this paper, OSUD imaging method is introduced, modelled and experimentally demonstrated. Three CW lasers with different wavelengths are exploited for transient heating and silicon tubes filled with blue ink and water are used for proof-of-concept demonstration. The proposed OSUD imaging enables spectroscopic optical absorption imaging using multiple low-cost CW laser sources and an ultrasound pulser-receiver. With further development of this technology, e.g. adopting cheaper and compact laser diode system, it is possible to design a portable imaging device for real clinical applications. In the future work, more solid validations will be performed including *in vivo* animal experiments.

REFERENCES

[1] Gao, F., Feng, X. & Zheng, Y. Advanced photoacoustic and thermoacoustic sensing and imaging beyond pulsed absorption contrast. Journal of Optics 18, 074006 (2016).
[2] Wang, L. V. & Hu, S. Photoacoustic Tomography: In Vivo Imaging from Organelles to Organs. Science 335, 1458-1462, (2012).
[3] Beard, P. Biomedical photoacoustic imaging. Interface Focus 1, 602-631 (2011).
[4] Wang, L. V. Multiscale photoacoustic microscopy and computed tomography. Nature Photonics 3, 503-509, (2009).
[5] Xu, M. H. & Wang, L. H. V. Photoacoustic imaging in biomedicine. Review of Scientific Instruments 77, 041101 (2006).
[6] Ntziachristos, V., Ripoll, J., Wang, L. H. V. & Weissleder, R. Looking and listening to light: the evolution of whole-body photonic imaging. Nature Biotechnology 23, 313-320 (2005).
[7] Yao, J. J., Kaberniuk, A. A. & Li, L. Multiscale photoacoustic tomography using reversibly switchable bacterial phytochrome as a near-infrared photochromic probe. Nat Methods 13, 67-+ (2016).
[8] Wang, L. H. V. & Yao, J. J. A practical guide to photoacoustic tomography in the life sciences. Nat Methods 13, 627-638 (2016).
[9] Yao, J. J., Wang, L. & Yang, J. M. High-speed label-free functional photoacoustic microscopy of mouse brain in action. Nat Methods 12, 407-+ (2015).
[10] Razansky, D., Distel M. & Vinegoni, C. Multispectral opto-acoustic tomography of deep-seated fluorescent proteins in vivo. Nature Photonics 3, 412-417 (2009).
[11] Zhang, H. F., Maslov, K., Stoica, G. & Wang, L. V. Functional photoacoustic microscopy for high-resolution and noninvasive in vivo imaging. Nature Biotechnology 24, 848-851 (2006).
[12] Wang, X. D., Pang, Y. & Ku G. Noninvasive laser-induced photoacoustic tomography for structural and functional in vivo imaging of the brain. Nature Biotechnology 21, 803-806 (2003).
[13] Wang, T. H., Nandy, S., Salehi, H. S., Kumavor, P. D. & Zhu, Q. A low-cost photoacoustic microscopy system with a laser diode excitation. Biomed Opt Express 5, 3053-3058 (2014).

[14] Zeng, L. M., Liu, G. D., Yang, D. W. & Ji, X. R. Portable optical-resolution photoacoustic microscopy with a pulsed laser diode excitation. Appl Phys Lett 102 (2013).
[15] Wang, L. V. Tutorial on Photoacoustic Microscopy and Computed Tomography. Selected Topics in Quantum Electronics, IEEE Journal of 14, 171-179 (2008).
[16] J. P. Wilkinson, Nonlinear resonant circuit devices (Patent style), U.S. Patent 3 624 12, July 16, 1990.
[17] Choi, C., Ahn, J. & Kim C. Photothermal strain imaging. Journal of Biomedical Optics 22.7(2017):76005.
[18] Shah, J., Aglyamov, S. R. & Sokolov, K. Ultrasound imaging to monitor photothermal therapy - feasibility study. Optics Express 16.6 (2008):3776-85.
[19] Liu, Dalong, & E. S. Ebbini. Real-Time 2-D Temperature Imaging Using Ultrasound. IEEE Trans Biomed Eng 57.1 (2010):12-6.
[20] Maass‐Moreno, Roberto, & C. A. Damianou. Noninvasive temperature estimation in tissue via ultrasound echo‐shifts. Part I. Analytical model.Journal of the Acoustical Society of America, 100.1 (1996):2514-2521.
[21] Petty, Charles C., & J. A. Curcio. The Near Infrared Absorption Spectrum of Liquid Water. Journal of the Optical Society of America, 41.5 (1951):302-304.
[22] O'Donnell, M., Skovoroda A. R. & Shapo B. M. "Internal displacement and strain imaging using ultrasonic speckle tracking." *IEEE Transactions on Ultrasonics Ferroelectrics & Frequency Control* 41.3(2002):314-325.
[23] Techavipoo, U., Varghese, T., Chen, Q., Stiles, T. A., Zagzebski, J. A., & Frank, G. R. "Temperature dependence of ultrasonic propagation speed and attenuation in excised canine liver tissue measured using transmitted and reflected pulses." *Journal of the Acoustical Society of America*, *115*(6), 2859.
[24] Bamber, J. C., and C. R. Hill. "Ultrasonic attenuation and propagation speed in mammalian tissues as a function of temperature." *Ultrasound in Medicine & Biology*, 5.2(1979):149.
[25] Li, P. C., and W. N. Lee. "An efficient speckle tracking algorithm for ultrasonic imaging." *Ultrason Imaging* 24.4(2002):215-228.
[26] Horstmeyer, R, H. Ruan, and C. Yang. "Guidestar-assisted wavefront-shaping methods for focusing light into biological tissue. " *Nature Photonics* 9.9(2015):563-571.
[27] Lai, P., Wang, L. Jian, W. T. & L. V. Wang "Photoacoustically guided wavefront shaping for enhanced optical focusing in scattering media." *Nature Photonics* 9.2 (2015):126.
[28] Tzoumas, S., Nunes, A., Olefir, I., Stangl, S., Symvoulidis, P., & Glasl, S. "Eigenspectra optoacoustic tomography achieves quantitative blood oxygenation imaging deep in tissues." *Nature Communications* 7.7(2016):12121.

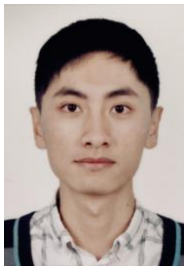

Tingyang Duan received his B.S. degree in Microelectronics and Solid State Electronics from University of Electronic Science and Technology of China in 2016. He is now a PhD candidate at School of Information Science and Technology in Shanghaitech University. His research interests focus on the development of PAM (photoacoustic microscope) imaging system and its biomedical applications. His recent research project is to combine Microfluidic chips and PAM system for fluid parameter measurement.

Hengrong Lan received his bachelor degree in Electrical Engineering from Fujian Agriculture and Forestry University in 2017. He is pursuing his degree of Master in ShanghaiTech University. His research interests are the biomedical and clinical image reconstruction, machine learning in photoacoustic and photoacoustic tomography systems design.

Hongtao Zhong has received his bachelor degree in Electrical Engineering from Guangzhou University, Guangzhou, China in 2017. He is a graduate student in HiSys Lab of ShanghaiTech University. His research interest is portable photoacoustic imaging device.

Meng Zhou received her B.S degree in biomedical engineering from Beijing Institute of Technology in 2016 and is now pursuing her Master's degree in Shanghaitech University. She is interested in image processing. In 2017, she jointed Spreadtrum communication company as image processing internship during the summer vacation. Her research interests are medical image processing and photoacoustic imaging techniques.

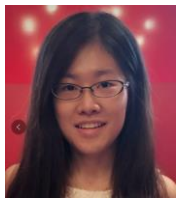

Ruochong Zhang received her B.S. degree from Nanyang Technological University, School of Electrical and Electronic Engineering in 2015. She is currently a PhD candidate and her research topic covers electromagnetic-acoustic sensing and imaging for biomedical applications.

Fei Gao (M'12**)** received his B.S. degree in electrical engineering from Xi'an Jiaotong University, Xi'an, China in 2009. He received the PhD degree in electrical and electronic engineering at Nanyang Technological University, in 2015. He was a postdoctoral visiting scholar at Stanford University in 2015. After that, he joined NTU working as a research fellow and electromagnetic-ultrasound group leader. He joined ShanghaiTech University as an assistant professor in Jan. 2017. His research interests include fundamental study and system development of thermoacoustic and photoacoustic imaging modalities, circuit and system for biomedical applications. He has authored and co-authored over 50 journal and conference papers, one book, one book chapter, and four patents filed.